COMPUTER SCIENCE TECHNICAL REPORT SERIES

UNIVERSITY OF MARYLAND
COLLEGE PARK, MARYLAND
20742

(1)

(9) Technical rept.,

(14) TR-559

(11) July 1977

(15) DAAG53-76C-0138, ARPA Order-3206

(12) 44p.

(6) STATISTICAL PROPERTIES OF THRESHOLDED IMAGES.

(10) Durga P. Panda
Computer Science Center
University of Maryland
College Park, MD 20742

ABSTRACT

The threshold operator is an important operator in image analysis tasks such as segmentation and edge detection. A statistical analysis of the response of this operator is presented in this paper. The input grayscale image is modelled as a two-dimensional homogeneous random process completely characterized by its mean and power spectrum.

The support of the U. S. Army Night Vision Laboratory under Contract DAAG53-76C-0138 (ARPA Order 3206) is gratefully acknowledged, as is the help of Mrs. Shelly Rowe in preparing this paper.

1473

403018

1. Introduction

Thresholding has played an important role in image processing. A grayscale image of a scene is thresholded to dichotomize the image into (for example) object and background points [1]. An edge picture can be thresholded to produce a binary edge picture corresponding to the binary decision of edge or no edge at a pixel. Binary representation of images, for storage and data compression, is achieved by nonuniform dynamic thresholding [2]. Nonuniform thresholding is also used to extract objects when uniform thresholding is inadequate [3]. Statistical analysis of the response of the threshold operator can be used, for example, in the error analysis of edge detection, in determining buffer size requirements for connected component analysis [4], or in determining the statistics of "edge/border coincidence" in a picture at a given threshold [5]. In this paper we discuss some statistical properties of uniformly thresholded grayscale images.

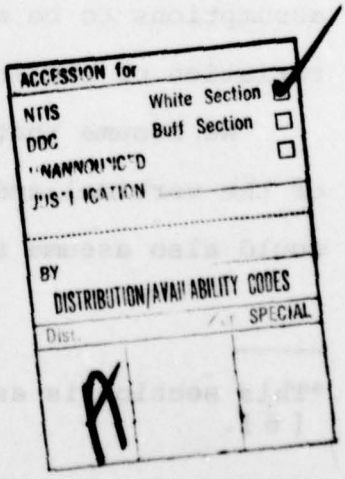

2. The input image*

In order to analyze the outputs of image operators we must have a statistical characterization of the input image. Often-used assumptions that the intensities or gray levels in an image are independent and identically distributed, or that an image is a sequence of single-parameter processes, are inadequate. An image is inherently a two-dimensional spatial process and hence should be treated as such. The literature in the area of two-dimensional processes is not as rich as in the area of one-dimensional processes. A few spatial processes other than images have received some attention from mathematicians. Examples of such processes that may have some relevance to image processing are the random surfaces encountered in sea waves [7], crop yield as a function of spatial location [8], and the height field of a portion of the earth's surface [9]. Fortunately, most of the assumptions made in the analysis of the spatial processes can be reasonably applied to images. Many of these assumptions are necessary for tractability. We shall now summarize the assumptions to be made here regarding the statistical characteristics of the input image.

We assume that the image gray level $z(x,y)$ is a function of the vertical and the horizontal coordinates, x and y. We could also assume that z is a function of time t. The rele-

---

*This section is essentially the same as part of Section 1 of [6].

vance of the time parameter t would be obvious if we were dealing with the dynamic behavior of an image, as in tracking a moving object in a scene. However, we shall be concerned only with static images here, and the dependence of z on t will, therefore, be dropped.

We shall also assume that the parameters x and y and the gray level z itself are continuous real variables. Furthermore, it is assumed that the random field can be represented as a sum of periodic functions:

$$z(x,y) = \sum_n a_n \cos(2\pi f_{n,x} x + 2\pi f_{n,y} y + \theta_n)$$

where $f_{n,x}$ and $f_{n,y}$ are the horizontal and vertical spatial frequencies, a_n is the random amplitude, and θ_n is the random phase, uniform distributed in $(0,2\pi)$. By the Central Limit Theorem, $z(x,y)$ is normally distributed and is assumed stationary. The assumption of stationarity implies that the first and second moments are independent of translation and rotation of the spatial coordinate axes. By imposing this restriction we exclude from further consideration the class of images called context dependent ensembles [10] where specific objects appear at approximately fixed locations. Hunt's example of such an ensemble [10] is the set of facial portraits taken for driver's license photographs, where objects such as the nose, the eyes, etc. appear at approximately the same locations in every picture, so that the mean gray level for such an ensemble is definitely a function of the spatial coordinates. In our case, however, we will assume that even if

objects occur in our images, they can occur in any positions, and have any orientations, sizes, and shapes.

Thus for the image ensembles that we will be considering, the marginal pdf of the gray level is

$$p(z(x,y)) = \frac{1}{\sqrt{2\pi}\sigma_z} \exp\left[-\frac{(z-\mu_z)^2}{2\sigma_z^2}\right]$$

where μ_z and σ_z are the mean and the standard deviation of $z(x,y)$. Strictly speaking, a normal distribution is inappropriate for image gray level, which is nonnegative. The problem is alleviated if we assume that the mean is much larger than the standard deviation. The value of the mean is, however, irrelevant in many applications, such as determining the autocovariance function of the input image. We shall assume, except when we need certain results explicitly in terms of μ_z, that the mean has been subtracted from the process $z(x,y)$. We also assume that the autocovariance $R_z(x,y)$ of z and its Fourier transform, the power spectrum $S_z(f_x,f_y)$, have derivations of all orders required in the analysis.

We define, for later use, the general (i,j)th order moment of a spectral density $S(f_x,f_y)$:

$$m(i,j) = \int_{-\infty}^{\infty}\int_{-\infty}^{\infty} S(f_x,f_y)\, f_x^i f_y^j \, df_x \, df_y.$$

In particular, the moments of the input spectral density are

$$m_z(i,j) = \iint S_z(f_x,f_y)\, f_x^i f_y^j \, df_x \, df_y.$$

When (i+j) is odd $m_z(i,j)$ is zero for a real process, since the spectral density is even. When (i+j) is even

$$m_z(i,j) = (-1)^{(i+j)/2} \frac{\partial^{i+1}}{\partial x^i \partial y^j} R_z(0,0). \tag{1}$$

The above implies that the moments $m(\cdot)$ satisfy the following relationship:

$$E\left[\frac{\partial^c z}{\partial x^a \partial y^{c-a}} \cdot \frac{\partial^d z}{\partial x^b \partial y^{d-b}}\right] = (-1)^{\frac{d-c}{2}} m_z(a+b,(c+d)-(a+b))$$

where a,b,c, and d are positive integers such that c>a, d>b, and c(mod2) = d(mod2) (i.e., c = d±2n, n being an integer). The following is a partial list of the moments for (c+d) ≤ 2:

$$m_z(0,0) = \sigma_z^2 \tag{2a}$$

$$m_z(2,0) = E\left[\frac{\partial z}{\partial x}\right]^2$$

$$= -E\left[z \cdot \frac{\partial^2 z}{\partial x^2}\right] \tag{2b}$$

$$m_z(0,2) = E\left[\frac{\partial z}{\partial y}\right]^2$$

$$= -E\left[z \cdot \frac{\partial^2 z}{\partial y^2}\right] . \tag{2c}$$

A longer list may be found in [6].

3. Theoretical analysis of the output

In thresholding, all points (x,y) with gray level z(x,y) above the threshold z_0 become black (say) and the rest white. The result is a binary image consisting of white background surrounding patches, or connected components, of black points, that are candidate regions in the segmentation process [1]. We shall derive some statistical properties of the thresholded binary image. These properties include moments (Section 3.1); density of border points (Section 3.2); and number of connected components (Section 3.3). The material in this section closely follows the treatments in [7 ,11].

3.1 Moments of the thresholded image

We shall adopt the convention that the gray level of a black point in the thresholded image is unity and that of a white point is zero. If w(x,y) is the thresholded image then

$$w(x,y) = \begin{cases} 1 \text{ if } z(x,y) > z_0 \\ 0 \text{ otherwise.} \end{cases} \tag{3}$$

The probability that a point in the thresholded image is black is

$$P(b) = Pr(w(x,y) = 1)$$

$$= \int_{z_0}^{\infty} \frac{1}{\sqrt{2\pi}\sigma_z} \exp[-\frac{(z-\mu_z)^2}{2\sigma_z^2}]$$

$$= 1-\varphi\left(\frac{z_0-\mu_z}{\sigma_z}\right)$$

where $\varphi(z)$ is the cdf of a zero-mean unit-variance normal variable,

$$\varphi(z) = \frac{1}{\sqrt{2\pi}} \int_{-\infty}^{z} \exp(-\xi^2/2)\, d\xi.$$

The first moment is simply

$$E[w(x,y)] = P(b)$$

$$= 1-\varphi\left(\frac{z_0-\mu_z}{\sigma_z}\right).$$

To determine the autocorrelation we make use of the following result due to Price [12,13]. If two zero mean unit-variance Gaussian variables z_1 and z_2, with cross-correlation coefficient

ρ_i, are nonlinearly transformed to $f_1(z_1)$ and $f_2(z_2)$, respectively, then the output correlation ρ_0 is given by

$$\frac{\partial \rho_0}{\partial \rho_i} = E[\frac{d}{dz_1} f_1(z_1) \frac{d}{dz_2} f_2(z_2)]. \tag{4}$$

It is easily seen that if z'(x,y) is a zero-mean unit variance Gaussian field then w(x,y) of eqn. (3) is obtained by the following relationship:

$$w(x,y) = \begin{cases} 1 \text{ if } z'(x,y) > \frac{z_0-\mu_z}{\sigma_z} \\ 0 \text{ otherwise.} \end{cases} \tag{5}$$

Clearly z' can be obtained from z by the relationship $z' = (z-\mu_z)/\sigma_z$, and has the same correlation coefficient as z. If

$$z_1 = z'(x',y')$$

$$z_2 = z'(x'+x,y'+y)$$

$$f_1(z') = f_2(z') = w$$

$$\rho_i = E[z_1,z_2]$$

$$= R_{z'}(x,y)$$

$$= \frac{1}{\sigma_z^2} R_z(x,y)$$

$$\rho_0 = E[f_1(z_1)\ f_2(z_2)]$$

$$= R_w(x,y) + E^2[w]$$

From eqn. (5)

$$\frac{d}{dz_1} f_1(z_1) = \delta(z_1 - z_0')$$

$$\frac{d}{dz_2} f_2(z_2) = \delta(z_2 - z_0')$$

where δ is the Dirac delta function, and z_0' is a shorthand notation for $(z_0 - \mu_z)/\sigma_z$. Thus, from (4)

$$\frac{\partial \rho_0}{\partial \rho_i} = E[\delta(z_1 - z_0')\ \delta(z_2 - z_0')]$$

$$= \frac{1}{2\pi\sqrt{1-\rho_i^2}} \exp[-\frac{z_0'^2}{(1+\rho_i)}].$$

When $\rho_i = 0$, ρ_0 is also zero. Therefore,

$$R_w(x,y) = \rho_0 + E^2(w)$$

$$= \frac{1}{2\pi} \int_0^{\rho_i} \frac{1}{\sqrt{1-\xi^2}} \exp[-\frac{(z_0-\mu_z)^2}{\sigma_z^2\ (1+\xi)}]\ d\xi$$

$$+ [1-\varphi(\frac{z_0-\mu_z}{\sigma_z})]^2.$$

Alternatively, the autocorrelation function ρ_0 can be obtained as follows:

$$\rho_0 = E[w(x',y')w(x'+x,y'+y)]$$

$$= Pr[w(x',y') = 1,\ w(x'+x,y'+y) = 1]$$

$$= Pr[z(x',y') > z_0,\ z(x'+x,y'+y) > z_0]$$

$$= 1 - P_{x,y}(z_0,\infty) - P_{x,y}(\infty,z_0) + P_{x,y}(z_0,z_0)$$

where $P_{x,y}$ is the joint cdf of z(0,0) and z(x,y). Thus ρ_0 is the integral of the joint pdf of z(0,0) and z(x,y) from z_0 to ∞. When (x,y) = (0,0) ρ_0 is the mean square value of the output binary image and is the same as the mean value of the image:

$$E[w^2] = 1-\varphi\left(\frac{z_0-\mu_z}{\sigma_2}\right)$$

$$\sigma_w^2 = E[w^2] - E^2[w]$$

$$= \varphi\left(\frac{z_0-\mu_z}{\sigma_z}\right)\ \left[1-\varphi\left(\frac{z_0-\mu_z}{\sigma_z}\right)\right].$$

3.2 Density of border points

We shall now obtain the expected density of border points in the binary image using certain results first obtained by Rice [14, 15] for one parameter processes and then extended to two dimensions by Longuet-Higgins [7]. Let us consider an infinitesimally small region $\varepsilon(x_0,y_0)$ arround a point (x_0,y_0) as shown in Figure 1. Since $\varepsilon(x_0,y_0)$ is small, we can assume that only one border passes through it. In the figure

dS = area of $\varepsilon(x_0,y_0)$

$\ell(A,B)$ = length of the portion of border intercepted by $\varepsilon(x_0,y_0)$ (at A and B).

α_0,θ_0 = magnitude α and direction θ of the gradient of the image at (x_0,y_0).

In order for the perimeter to pass through $\varepsilon(x_0,y_0)$, the gray level $z(x_0,y_0)$ must lie in a small interval (z_1,z_2) around the threshold z_0. As long as α and θ are constant, changing the gray level $z(x_0,y_0)$ in the range z_1 and z_2 will correspond to changing the normal n between n_1 and n_2 given by

$$z_1 - z_0 = \alpha n_1$$

$$z_2 - z_0 = \alpha n_2$$

$$\int_{n_1}^{n_2} \ell \, dn = dS.$$

The expected length of this portion (A,B) is

$$E[\ell(A,B)\,|\,\alpha,\theta] = \int_{z_1}^{z_2} \ell \; p(z|\alpha,\theta) \; dz$$

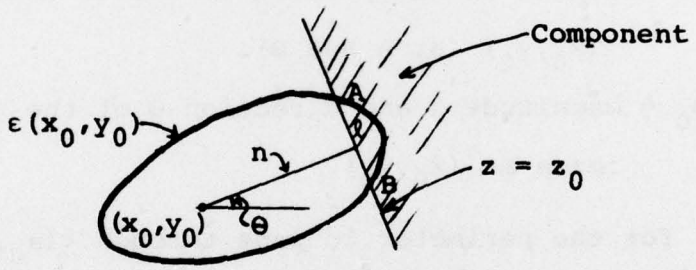

Figure 1. An incremental region $\varepsilon(x_0, y_0)$ around the point (x_0, y_0).

$$= \int_{n_1}^{n_2} \ell \; p(z_0|\alpha,\Theta)\alpha \; dn$$

$$E[\ell(A,B)] = E[E[\ell(A,B)|\alpha,\Theta]]$$

$$= \int_0^{\infty} \int_0^{2\pi} \int_{n_1}^{n_2} \ell \; p(z_0|\alpha,\Theta) \; \alpha \; dn \; p(\alpha,\Theta) \; d\Theta d\alpha$$

Since z is independent of $\frac{\partial z}{\partial x}$ and $\frac{\partial z}{\partial y}$ and

$$\alpha = \sqrt{\left(\frac{\partial z}{\partial x}\right)^2 + \left(\frac{\partial z}{\partial y}\right)^2}$$

$$\Theta = \tan^{-1}\left(\frac{\partial z}{\partial x}\right) / \left(\frac{\partial z}{\partial y}\right)$$

z is independent of α and Θ. So

$$E[\ell(A,B)] = p(z_0) \int_{n_1}^{n_2} \ell \; dn \; E[\alpha]$$

$$= p(z_0) \; dS \; E[\alpha]$$

from which

$$E[\ell] = p(z)E[\alpha] \int_S dS$$

$$= p(z_0) \; E[\alpha] \; HV \qquad (6)$$

where the image is assumed defined over a rectangular space S, and H and V are the horizontal and vertical dimensions of the image. Since z is normally distributed, so are $\frac{\partial z}{\partial x}$ and $\frac{\partial z}{\partial y}$. We can choose the axes of the coordinate system so that $\frac{\partial z}{\partial x}$ and $\frac{\partial z}{\partial y}$ are uncorrelated. If the image is isotropic then the variances of $\frac{\partial z}{\partial x}$ and $\frac{\partial z}{\partial y}$ are the same and in such case α is

Rayleigh distributed. Hence

$$E[\alpha] = \sqrt{\frac{\pi}{2} R_{\frac{\partial z}{\partial x}}(0,0)}$$

$$= \sqrt{\frac{\pi}{2} m_z(2,0)} \qquad (7)$$

Substituting eqn. (7) in eqn. (6) we obtain

$$E[\ell] = \frac{1}{\sqrt{2\pi R_z(0,0)}} \exp[-(z_0-\mu)^2/2R_z(0,0)] \sqrt{\frac{\pi}{2} m_z(2,0)}\, HV$$

$$= \frac{HV}{2} \sqrt{\frac{m_z(2,0)}{m_z(0,0)}} \exp[-(z_0-\mu)^2/2m_z(0,0)]$$

keeping in mind that $m_z(2,0) = m_z(0,2)$. When the image is not isotropic $\frac{\partial z}{\partial x}$ and $\frac{\partial z}{\partial y}$ have unequal variance, i.e.,

$$m_z(2,0) \neq m_z(0,2)$$

and α is no longer Rayleigh distributed. The mean perimeter per unit area can be found to be (see [7])

$$E[\ell] = \frac{HV}{\pi} \sqrt{\frac{m_z(2,0)+m_z(0,2)}{m_z(0,0)}} \exp[-\frac{(z_0-\mu_z)^2}{2m_z(0,0)}]\, f(\gamma)$$

where γ is the ratio of the smaller to the larger of the two moments $m_z(2,0)$ and $m_z(0,2)$, i.e.,

$$\gamma = \frac{\min[m_z(2,0), m_z(0,2)]}{\max[m_z(2,0), m_z(0,2)]}$$

$$= \frac{m_z(2,0)+m_z(0,2) - |m_z(2,0)-m_z(0,2)|}{m_z(2,0)+m_z(0,2) + |m_z(2,0)+m_z(0,2)|}$$

$$f(\gamma) = \frac{F_1(\sqrt{1-\gamma^2})}{\sqrt{1+\gamma^2}}$$

$$F_1(k) = \int_0^{\pi/2} \sqrt{1-k^2\sin^2\theta}\ d\theta$$

which is Legendre's complete elliptic integral of the first kind. The value of γ can vary between 0 and 1. It has been shown [7] that $f(\gamma)$ does not depart much from unity for $0 \leq \gamma \leq 1$ increasing monotonically from $f(0) = 1$ to

$f(1) = \frac{\pi}{2\sqrt{2}} = 1.1107$. Thus, in general,

$$E(\ell) \simeq \frac{HV}{\pi}\sqrt{\frac{m_z(2,0)+m_z(0,2)}{m_z(0,0)}}\ \exp[-\frac{(z_0-\mu_z)^2}{2m_z(0,0)}].$$

3.3 Number of connected components

3.3.1 Number of connected components in a row

Let $C(z_0)$ be the average number of connected components in a row of the thresholded image. Figure 2 shows two examples of gray level fluctuations along a particular row $y = y_0$. In Figure 2a $z(0,y_0) < z_0$ and the number of components (number of shaded regions) $C_{y_0}(z_0)$ in the row y_0 is 2. In Figure 2b $z(0,y_0) > z_0$ and the number of components is 3. It is easily seen that

$$C_{y_0}(z_0) = N_{y_0}(z_0)/2 + \Psi$$

where $N_{y_0}(z_0)$ is the number of times the image crosses the gray level z_0 in the row y_0. The value of Ψ depends on $N_{y_0}(z_0)$ and $z(0,y_0)$. When $N_{y_0}(z_0)$ is odd Ψ is $\frac{1}{2}$; when $N_{y_0}(z_0)$ is even Ψ is 1 if $z(0,y_0) > z_0$, 0 if $z(0,y_0) < z_0$. Thus

$$C(z_0) = E[C_{y_0}(z_0)]$$

$$= \frac{1}{2} E[N_{y_0}(z_0)] + E[\Psi]$$

$$E[\Psi] = \frac{1}{2} Pr(N=odd) + Pr(N=even, z_\ell > z_0) \qquad (8)$$

where $N = N_{y_0}(z_0)$, $z_\ell = z(0,y_0)$. The probability of N being odd or even depends on the length of a row. If z_r is the gray level at the right end point of the y_0th row then

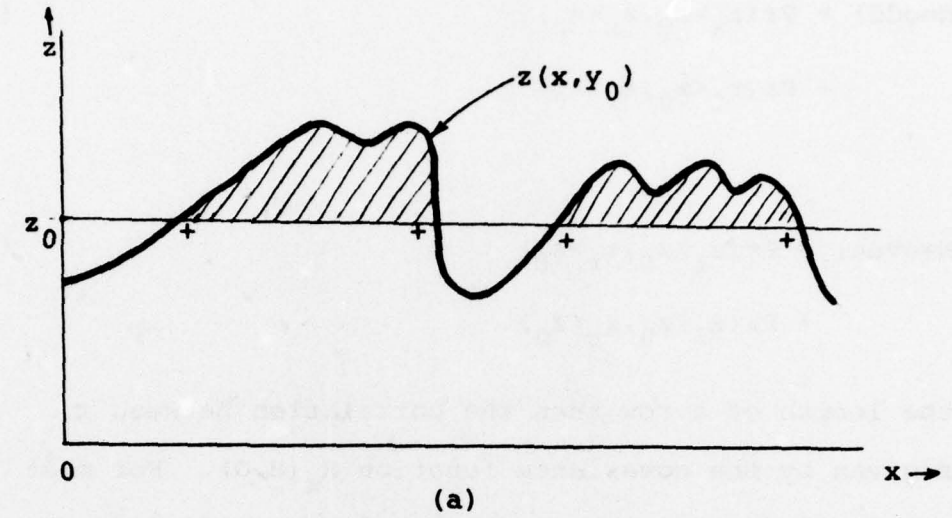

(a)

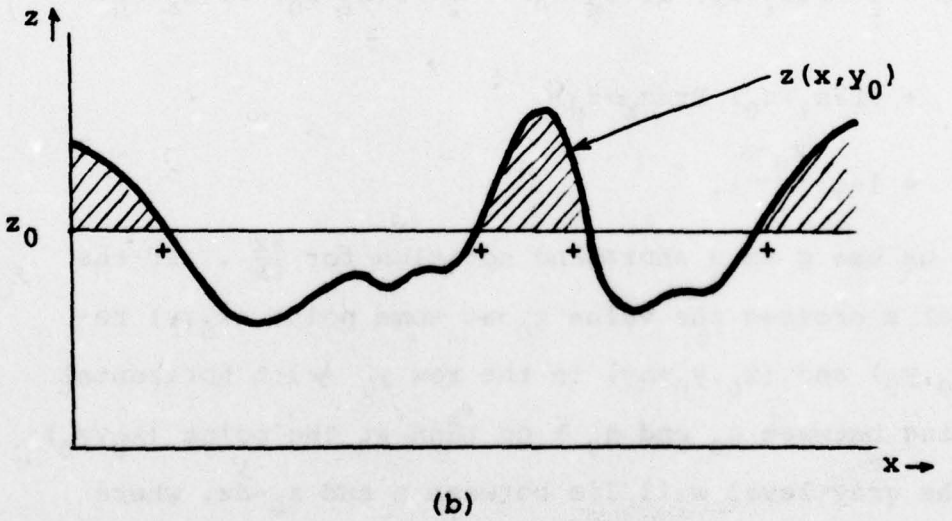

(b)

Figure 2. Two examples of gray level fluctuations along a row.

$$\Pr(N=\text{odd}) = \Pr(z_\ell > z_0, z_r < z_0) + \Pr(z_\ell < z_0, z_r > z_0) \tag{9a}$$

and

$$\Pr(N=\text{even}) = \Pr(z_\ell > z_0, z_r > z_0) + \Pr(z_\ell < z_0, z_r < z_0). \tag{9b}$$

If H is the length of a row then the correlation between z_ℓ and z_r is given by the covariance function $R_z(H,O)$. For most image processing applications, where H is large, $R_z(H,O)$ can be assumed to be zero. Therefore, the jointly normal random variables z_ℓ and z_r are independent, and from eqns. (8) and (9) we have

$$E[\Psi] = \tfrac{1}{2}\Pr(z_\ell > z_0)\Pr(z_r < z_0) + \tfrac{1}{2}\Pr(z_\ell < z_0)\Pr(z_r > z_0) + \Pr(z_\ell > z_0)\Pr(z_r > z_0)$$

$$= 1 - \varphi\left(\frac{z_0 - \mu}{\sigma}\right).$$

Let us use g as a shorthand notation for $\frac{\partial z}{\partial x}$. If the gray level z crosses the value z_0 at some point (x_0, y) between (x_0, y_0) and (x_0, y_0+dy) in the row y_0 with horizontal slope lying between g_0 and $g_0 + dg$ then at the point (x_0, y_0) itself the gray level will lie between z and z_0-dz, where

$$dz \simeq \frac{\partial z}{\partial x}\, dx \simeq g_0 dx.$$

The probability of getting this infinitesimal gray level

range at some point between (x_0,y_0) and (x_0+dx,y_0) is, assuming $g_0 \neq 0$,

$$p(z_0|g_0)\, dz = p(z_0|g_0)\, g_0 dx \,. \tag{10}$$

When g_0 is negative this probability is

$$-\, p(z_0|g_0)\, g_0 dx. \tag{11}$$

Combining eqn. (10) and eqn. (11) the probability is given by

$$p(z_0|g_0)\, |g_0|\, dx.$$

The probability of the gray level crossing the value z_0 between (x_0,y_0) and (x_0+dx,y_0) is

$$p_{z_0} = \int P(z_0|g_0)\, p(g_0)\, |g_0|\, dx\, dg.$$

Therefore, the total number of such gray level crossings between $(0,y_0)$ and (H,y_0) is

$$N_{y_0}(z_0) = \int_0^H p_{z_0}\, dx.$$

The cross-correlation between z and g is

$$E[z(x,y)g(x,y)] = R_{zg}(0,0)$$

$$= -\frac{\partial}{\partial x} R_z(0,0).$$

Since the autocorrelation function $R_z(x,y)$ is always symmetrical, $-\frac{\partial}{\partial x} R_z(0,0)$ is zero. Therefore, if the background image is normally distributed then z and $\frac{\partial z}{\partial x}$ are independent.

Thus

$$N_{y_0}(z_0) = p(z_0) \int_{-\infty}^{\infty} p(g_0)|g_0|dg \int_0^H dx$$

$$= p(z_0)E[|g_0|]\ H$$

$$= \frac{1}{\sqrt{2\pi}\sigma_z} e^{-\frac{1}{2}\left(\frac{z_0-\mu}{\sigma}\right)^2} \cdot \sqrt{\frac{2}{\pi}}\,\sigma_g\ H$$

$$= \frac{H}{\pi} \exp[-\ (z_0-\mu)^2/2m_z(0,0)]\ \sqrt{\frac{m_z(0,2)}{m_z(0,0)}}\ .$$

3.3.2 A lower bound on the number of connected components in the image

We shall now determine a lower bound on the average number of connected components in a thresholded binary image. Roach [16] has derived upper and lower bounds for this number when the points in the binary process are independent. In our case the points in the process are always correlated. We shall take the following approach to the problem. Let $C(z_0)$ and $H(z_0)$ be the average numbers of connected components and holes in a thresholded image. Suppose we traverse the perimeter of a component and measure the angle covered, with counterclockwise movement corresponding to positive angle. The traversal at the picture border is done in the manner shown in Figure 3 . For a component with no holes this angle is 2π. For a component with one hole the angle is 0, for a component with two holes the angle is -2π, and so on. In general the average total angle traversed is

$$E[\Xi(z_0)] = 2\pi[C(z_0) - H(z_0)]$$

$$\begin{cases} C(z_0) - H(z_0) = \frac{1}{2\pi} E[\Xi(z_0)] \\ C(z_0) \geq \frac{1}{2\pi} E[\Xi(z_0)] \end{cases}$$

For isotropic images the average $\Xi(z_0)$ is, following [11],

$$E[\Xi(z_0)] = HV \frac{m_z(0,2)}{(2\pi m_z(0,0))^{3/2}} (z_0-\mu) \exp\left(-\frac{(z_0-\mu)^2}{2m_z(0,0)}\right)$$

which is negative when $z_0 < \mu$. Since $C(z_0)$ is always non-negative a lower bound $L(z_0)$ on $C(z_0)$ is given by

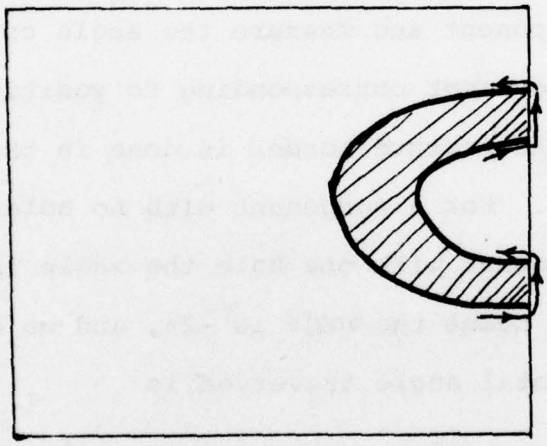

Figure 3. The convention of traversal along a component perimeter at the picture border.

$$L(z_0) = \frac{HVm_z(0,2)}{(2\pi\, m_z(0,0)^{3/2}}\,(z_0-\mu)\exp[-\frac{(z_0-\mu)^2}{2m_z(0,0)}]U(z_0-\mu)$$

where $U(\cdot)$ is the unit step function.

If we can estimate the average number of connected components, then we can use the results of Sections 3.1-2 to obtain estimates of the average area and perimeter of a connected component.

4. Comparison with measured data

In this section we compare some of the theoretical results of the last section with corresponding quantities measured from digitized and quantized test images. Four test images selected for this purpose are shown in Figure 4. Two of the test images, P1 and P2, show background regions selected from forward-looking infrared (FLIR) imagery. The third image, P3, is a computer-generated two-dimensional moving average (MA) process of order (2,2) [17], and the fourth image, P4, is a computer-generated white noise process. The images are 62x62 pixels in size, and have grayscale 0-63. Figure 5 shows the histograms of the test images. From these histograms the assumption of a normal pdf seems to be a reasonable one.

Each image is thresholded at several gray levels in its dynamic range and the number of border points in each thresholded image is counted. The average of the number of white border points and black border points is considered to be the number of border points in the thresholded image. This number is plotted against the probability of a black point, which is the ratio of black points to the total number of points, in each thresholded image. Corresponding to these thresholds the predicted number of border points and the predicted probabilities of black points are computed and plotted. The necessary moments of the spectral densities are estimated by substituting spatial averages for ensemble averages in eqn. (2). The graphs of the measured and predicted numbers

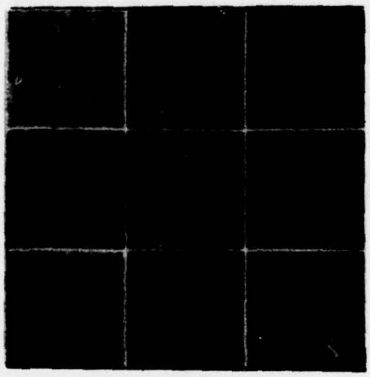

Figure 4. The four test images:
bottom right = P1, top right = P2,
top left = P3, and bottom left = P4.

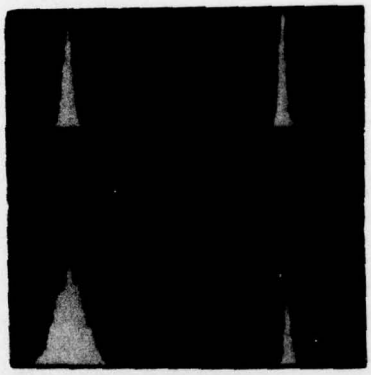

Figure 5. The histograms of the four test images in Figure 4.

of border points are shown in Figure 6 .

Similarly, the measured and the predicted average numbers of components per row are plotted as functions of the probabilities of black points for each of the test images. These graphs are shown in Figure 7 . Figure 8 shows the graphs of total numbers of components counted in the images compared with their predicted lower bounds.

The functional forms of the predicted and the measured quantities appear to be in good agreement with each other. The results on the numbers of components per row are especially encouraging. But, regarding the total number of components in the image, a tighter lower bound, for that matter, an upper bound, would be desirable.

Further theoretical as well as experimental work on classes of more complex images would be useful. Examples of such complex images may be textures whose pdfs are mixtures of two or more normal pdfs.

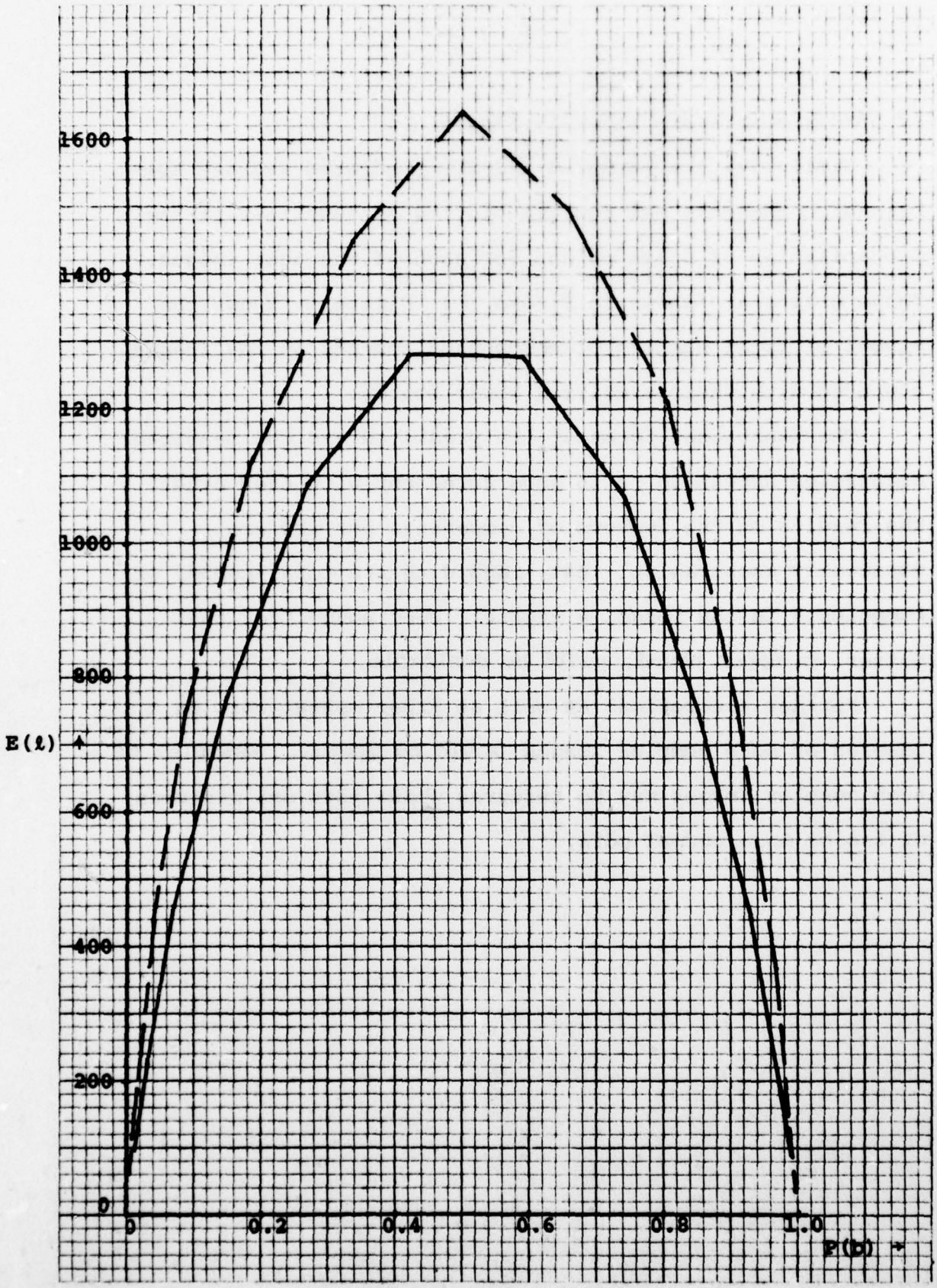

Figure 6. Number of border points as a function of P(b): solid lines = predicted values, dashed lines = measured data.

a. image P1.

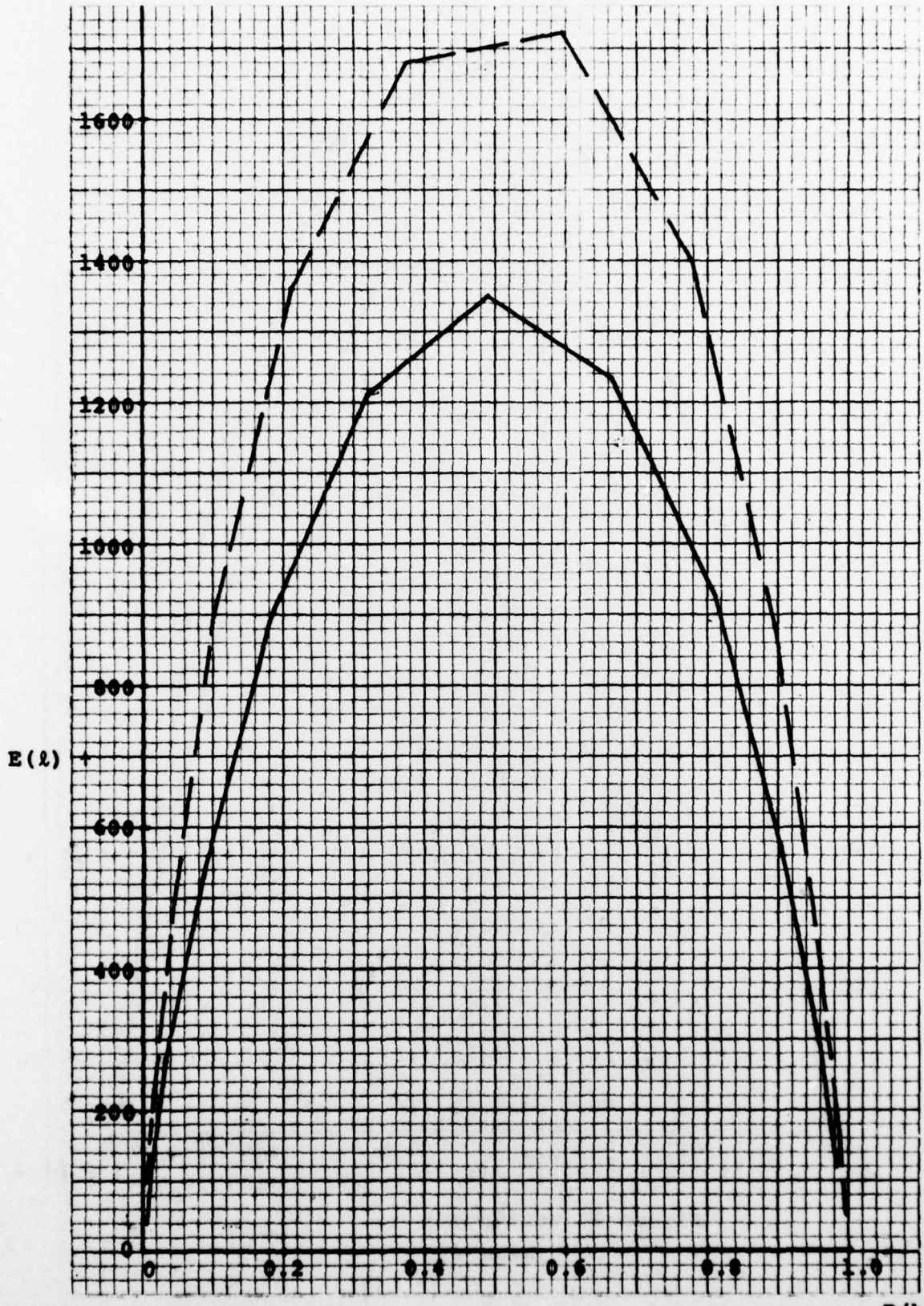

Figure 6 (continued)

b. image P2.

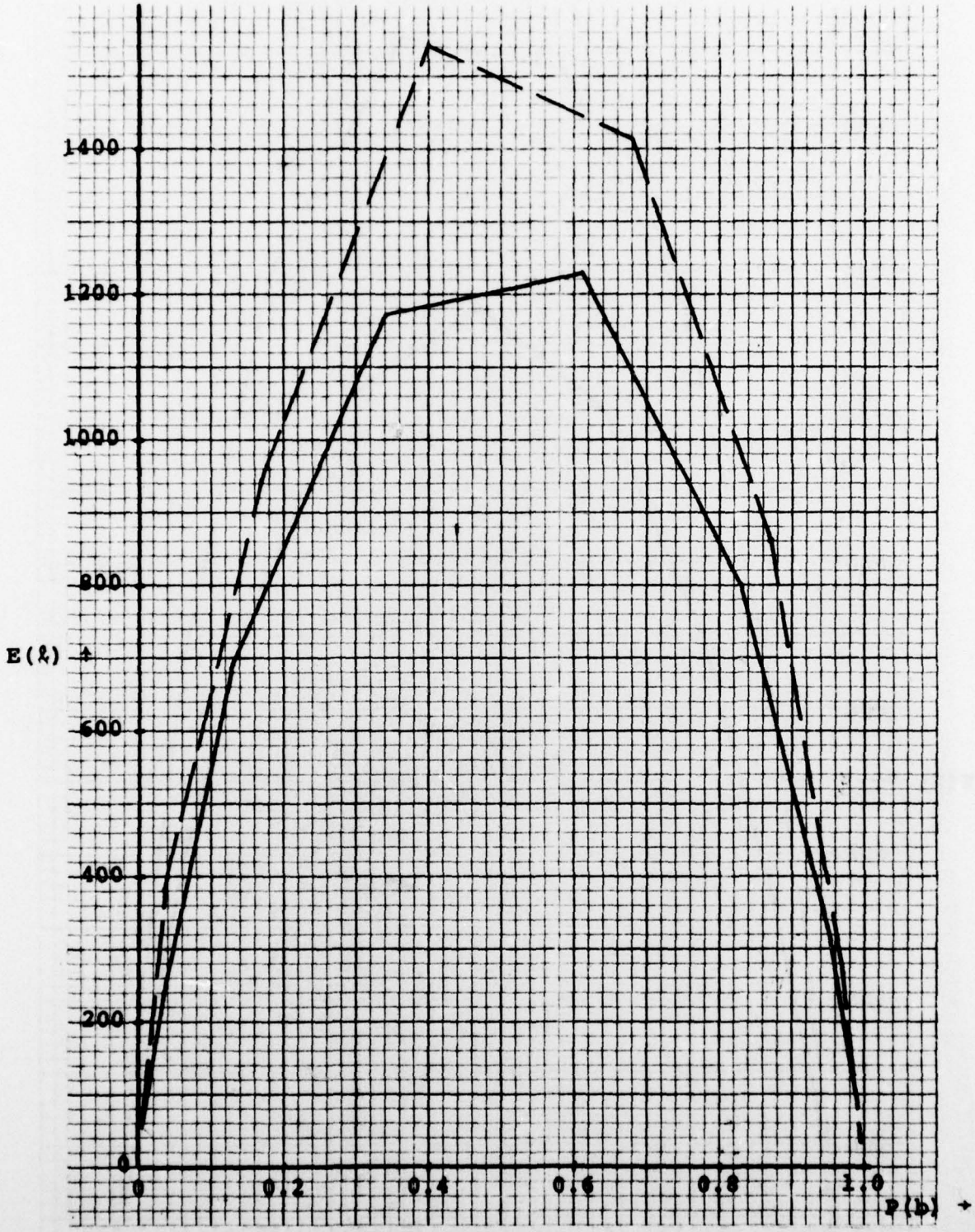

Figure 6 (continued)

c. image P3.

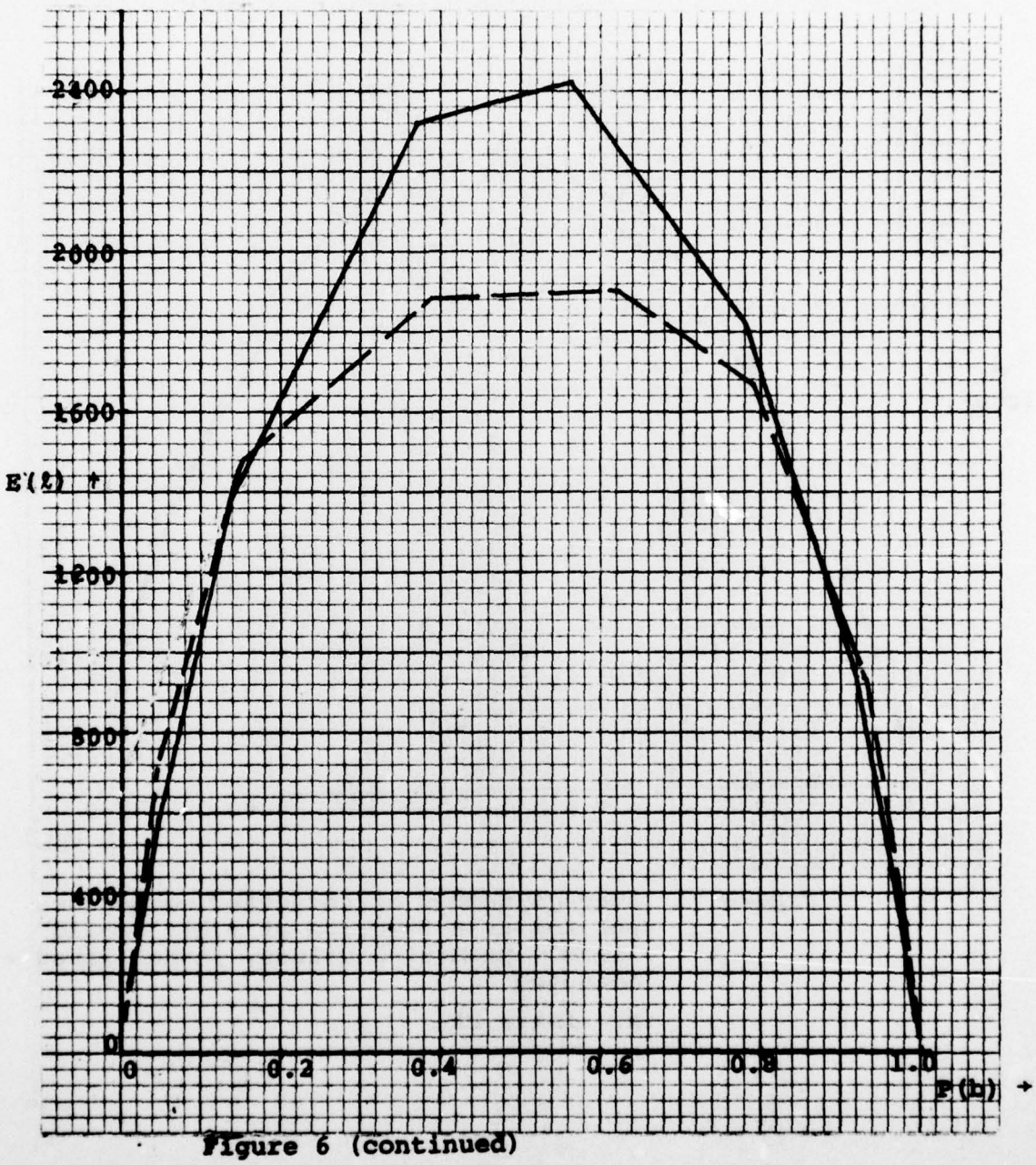

Figure 6 (continued)

d. image P4.

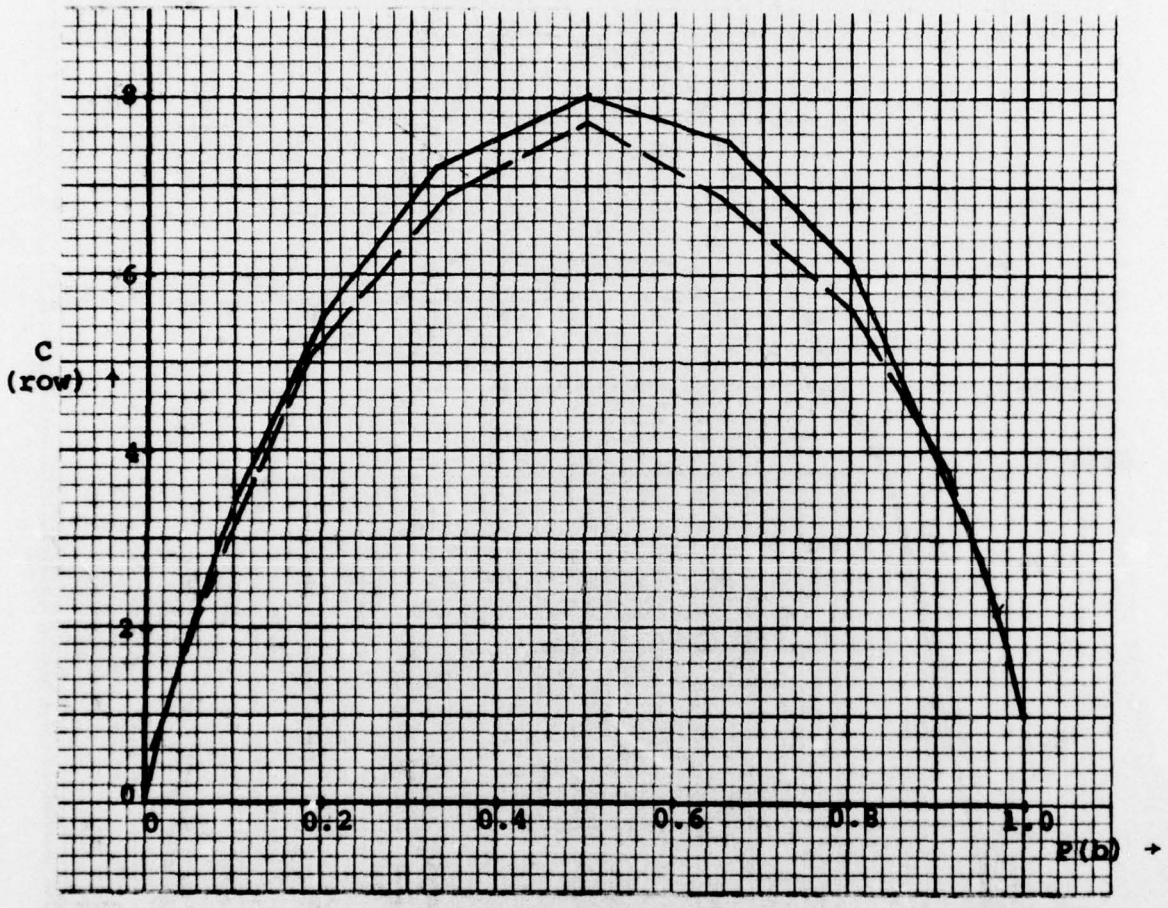

Figure 7. Average number of connected components per row as a function of P(b): solid lines = predicted values, dashed lines = measured

a. image P1.

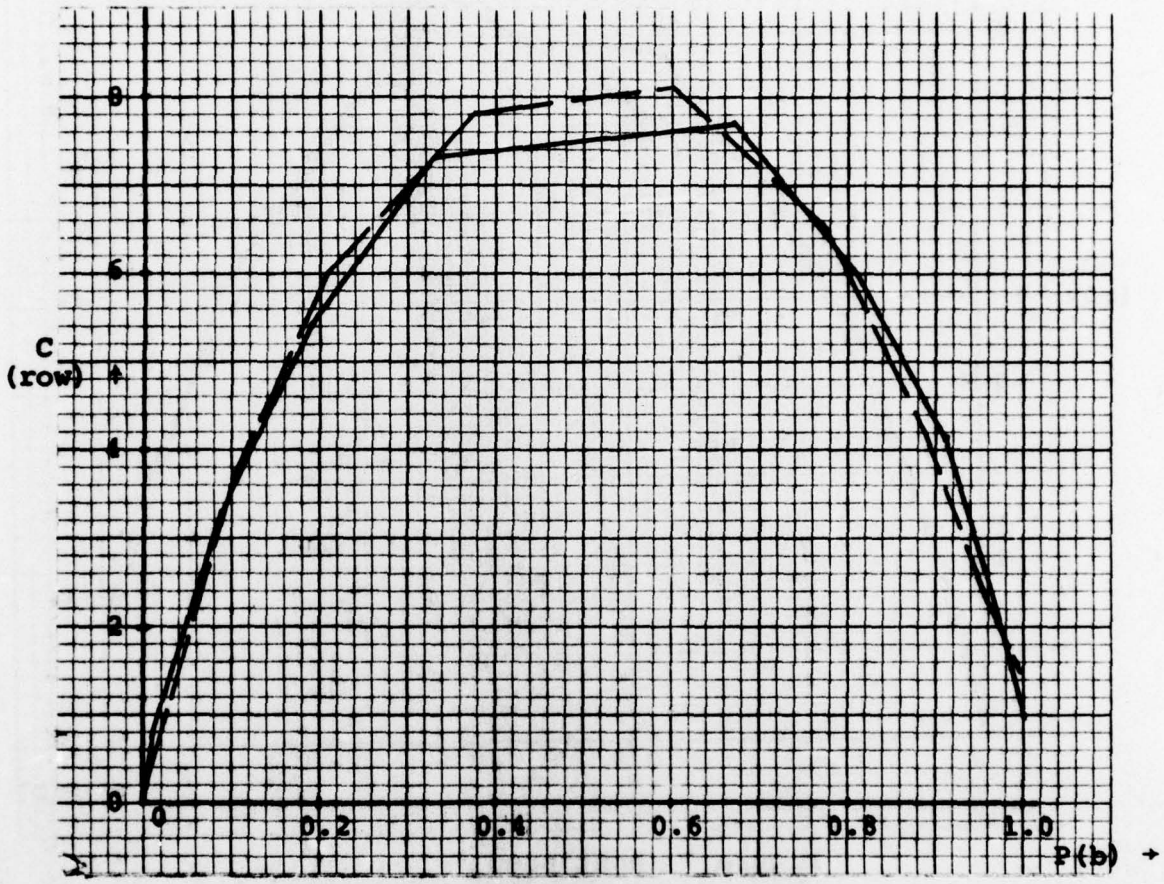

Figure 7 (continued)

b. image P2.

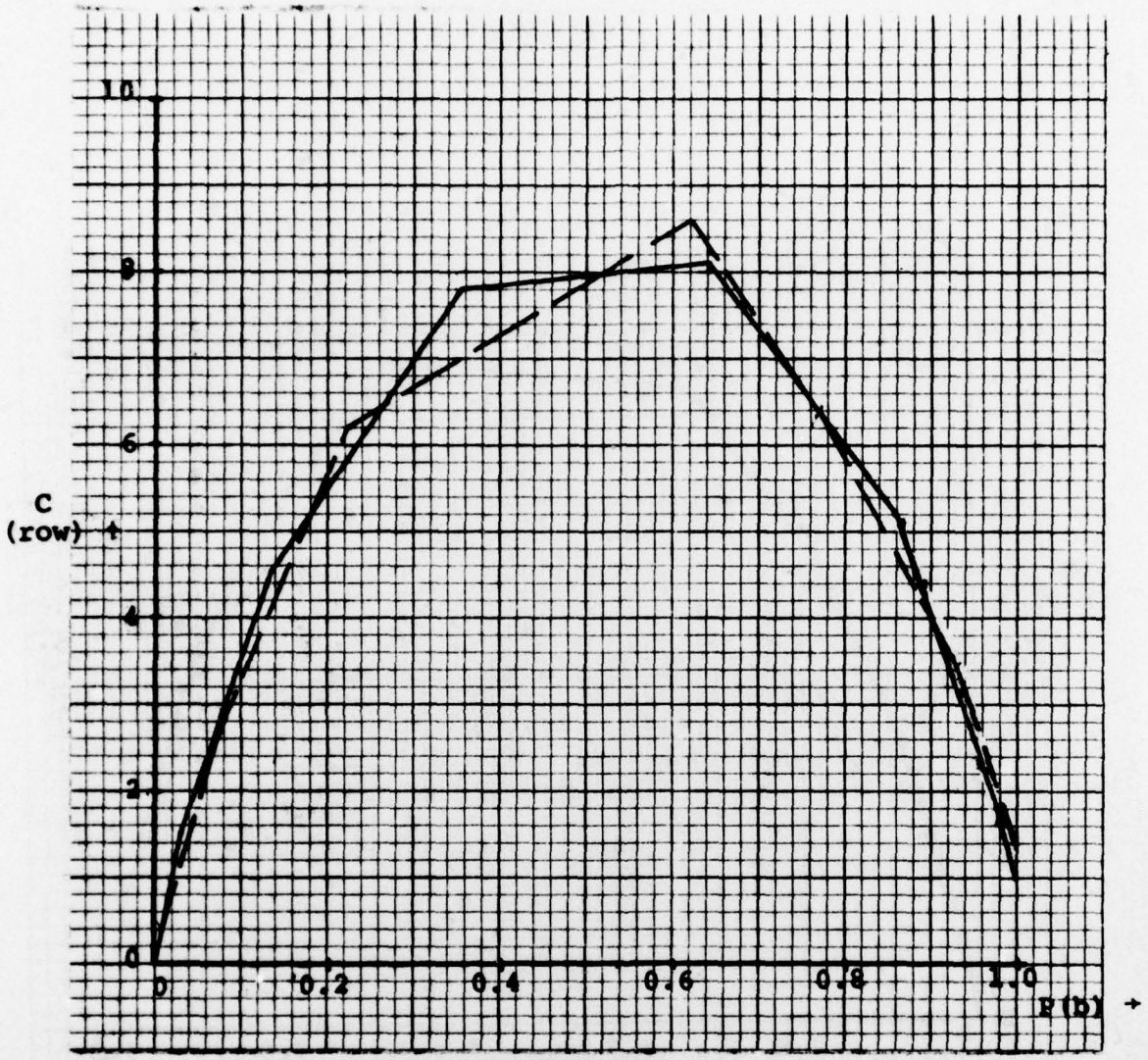

Figure 7 (continued)

c. image P3.

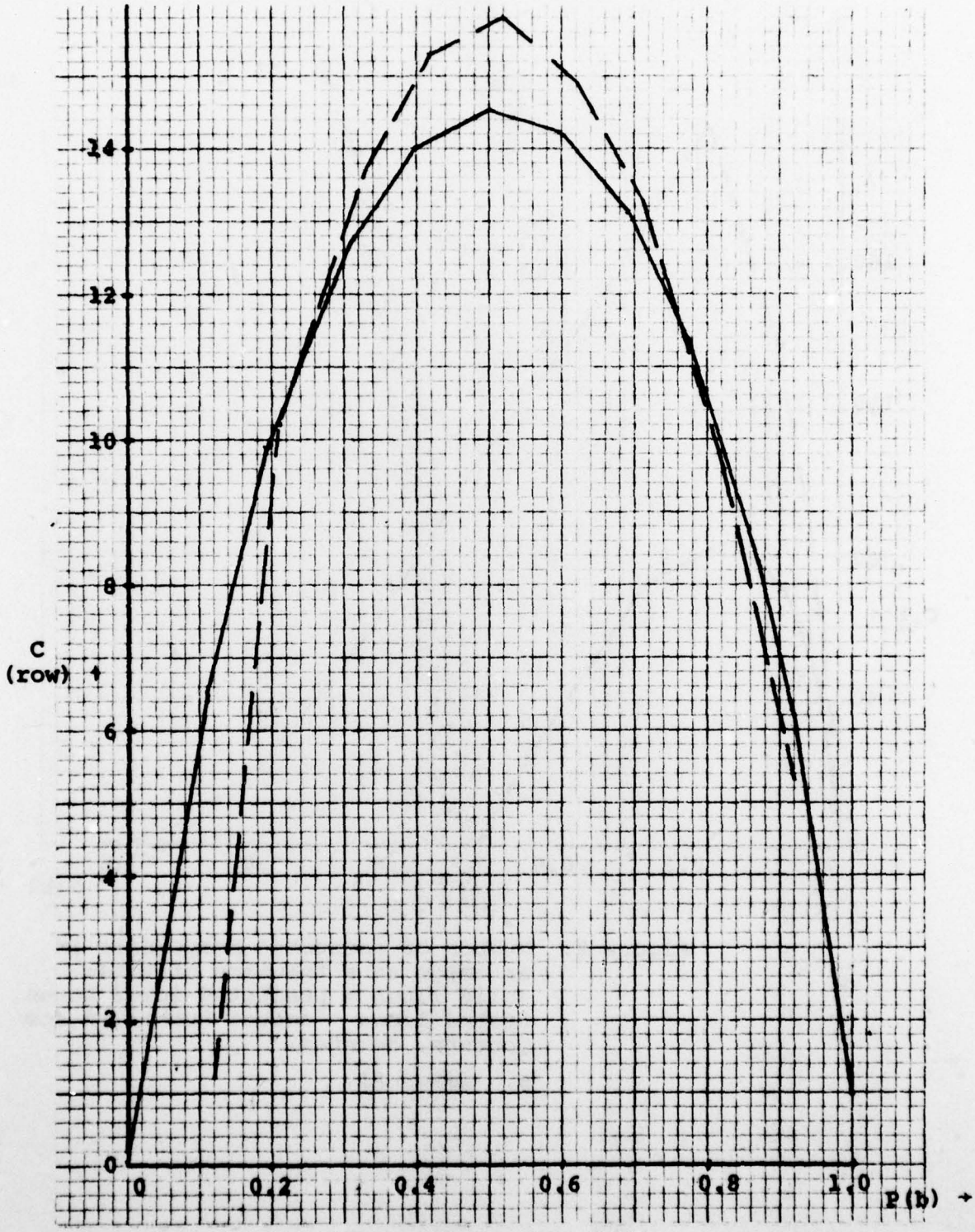

Figure 7 (continued)

d. image P4.

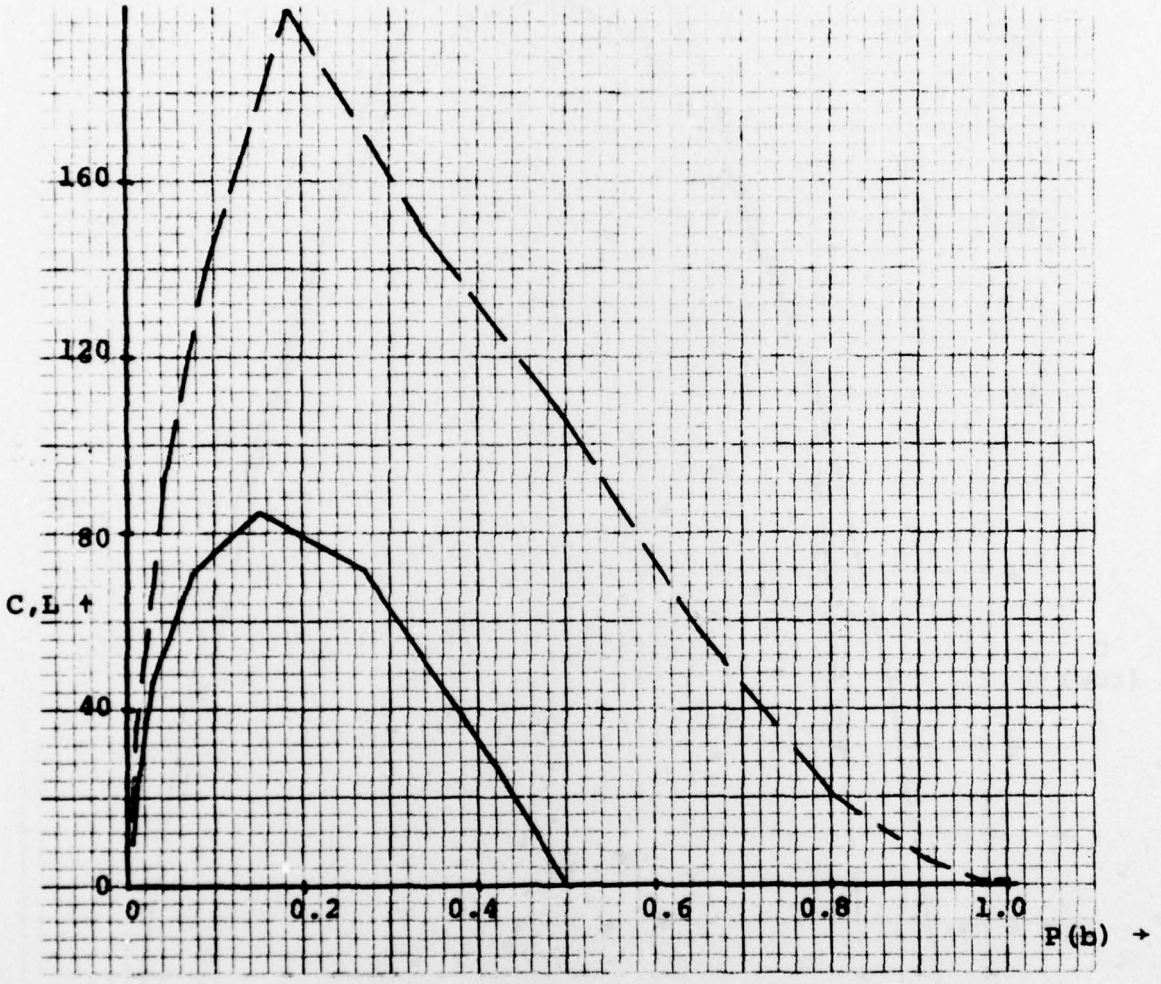

Figure 8. Number of connected components in an image as a function of P(b): solid lines = predicted lower bound, dashed lines = actual number of components, counted.

a. image P1.

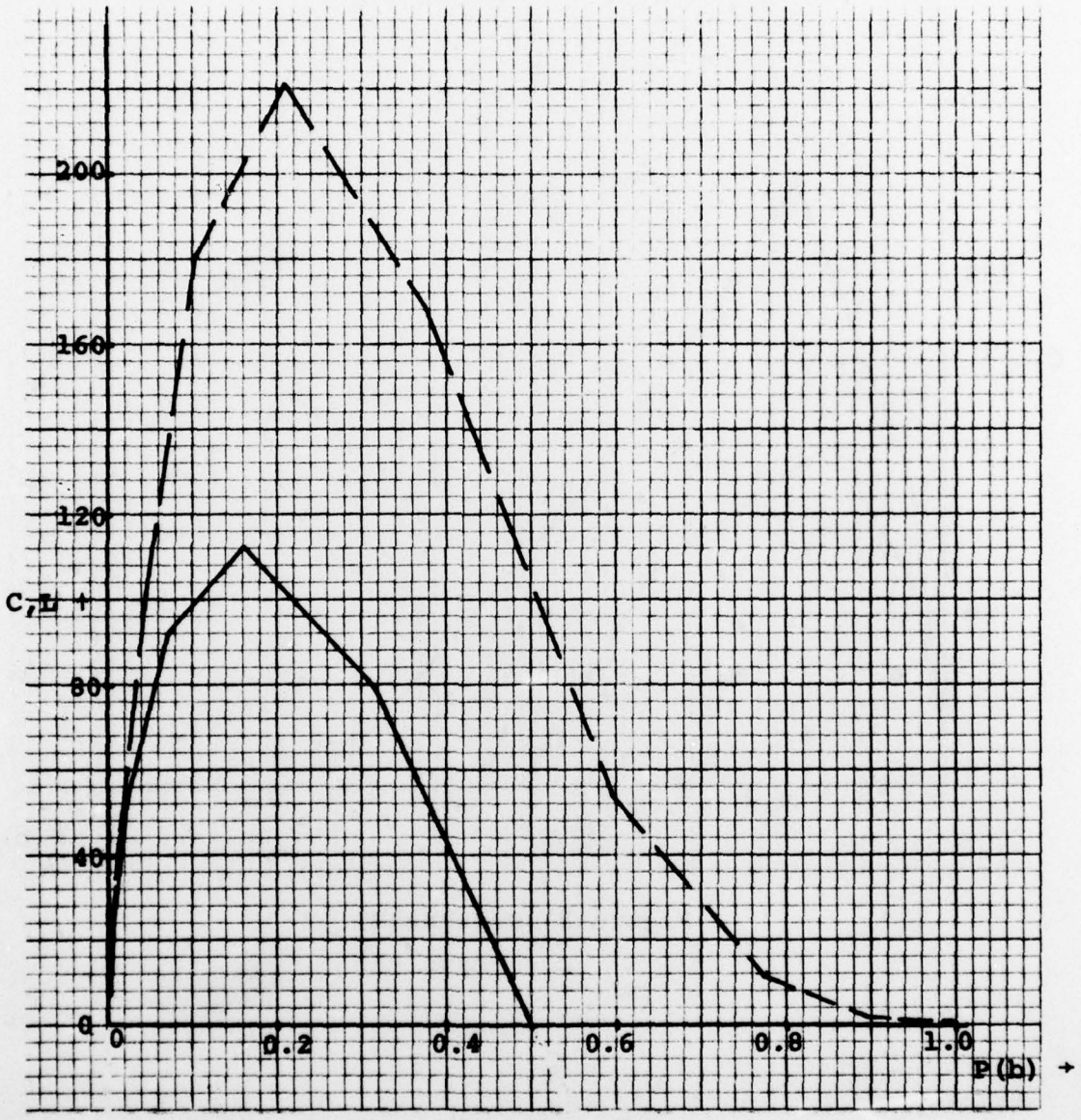

Figure 8 (continued)

b. image P2.

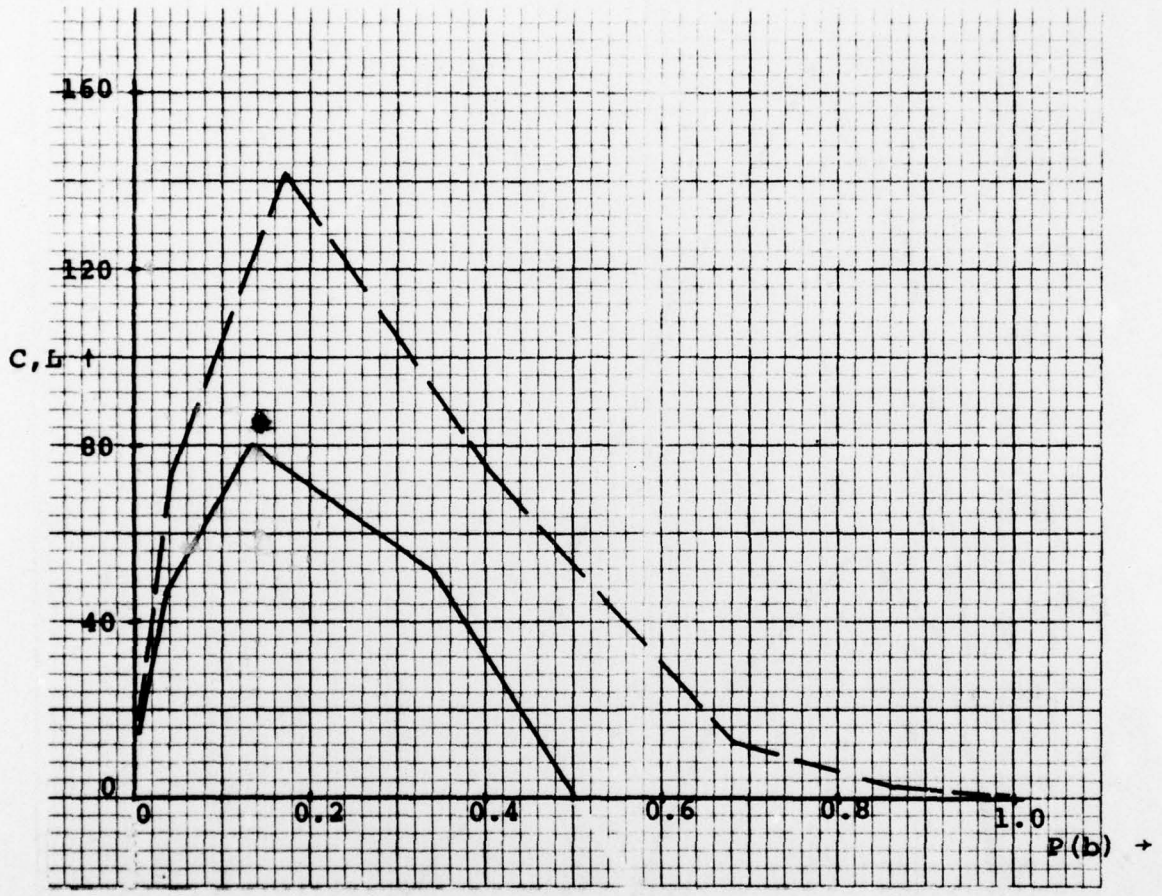

Figure 8 (continued)

c. image P3.

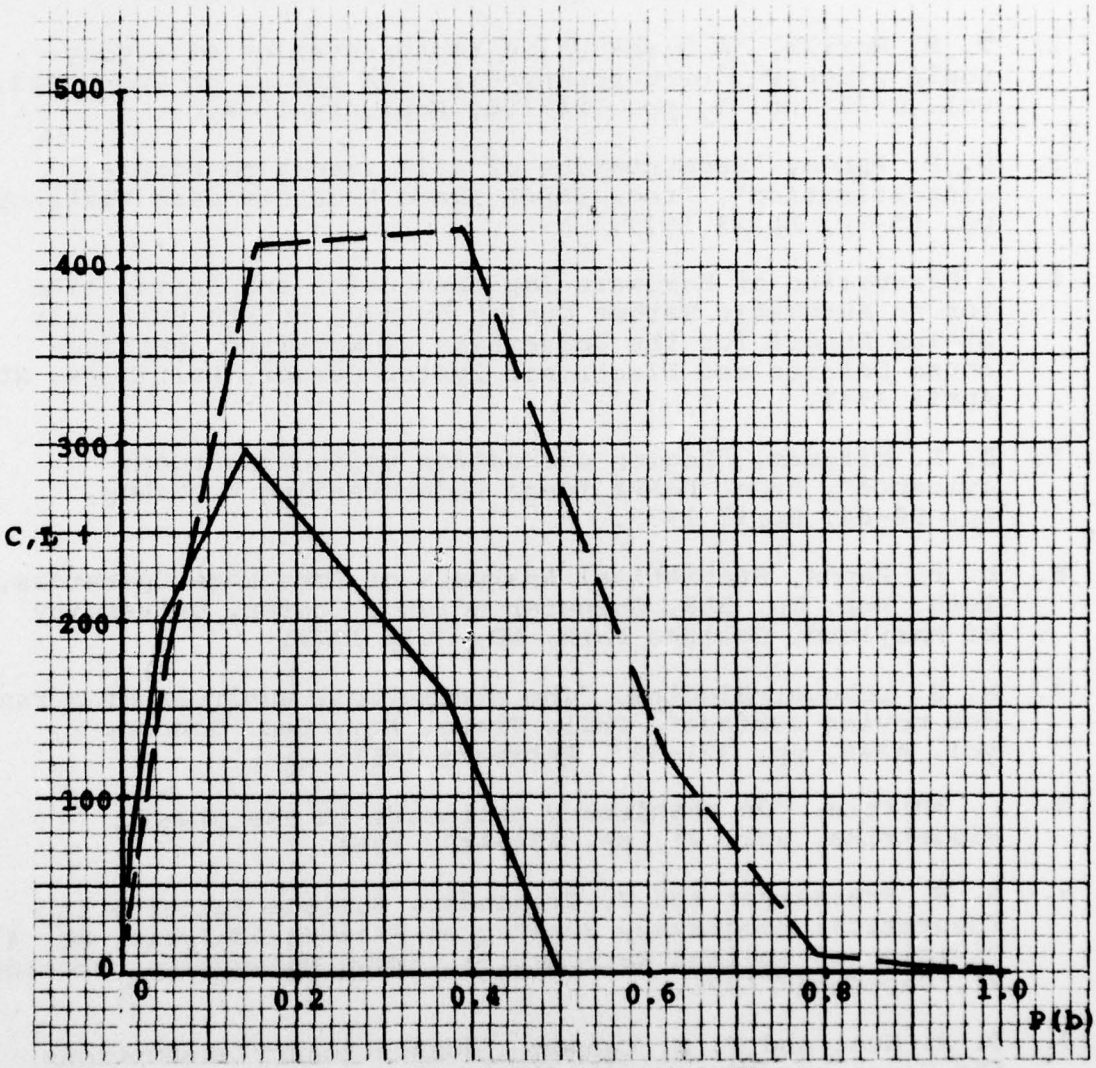

Figure 8 (continued)

d. image P4.

References

1. A. Rosenfeld and A. C. Kak, Digital Picture Processing, Academic Press, New York, 1976, Chapters 8 and 9.

2. T. H. Morrin, "A black-white representation of a gray-scale picture",(Correspondence), IEEE Trans. on Computers, vol. C-23, no. 2, pp. 184-186, February 1974.

3. D. P. Panda, "Segmentation of FLIR images by pixel classification", Proc. DARPA Image Understanding Workshop, pp. 65-70, April 1977.

4. A Discussion of Hardware Implementation and Fabrication for an Automatic Target Cueing System, Fourth Quarterly Status Report for the University of Maryland, Westinghouse Defense and Electronic System Center, Baltimore, MD, April 1977.

5. D. L. Milgram, "Region extraction using convergent evidence", Proc. DARPA Image Understanding Workshop, pp. 58-64, April 1977.

6. D. P. Panda, Statistical Analysis of Some Edge Operators, Tech. Rep. No. 558, Computer Science Center, University of Maryland, College Park, MD, July 1977.

7. M. S. Longuet-Higgins, "The statistical analysis of a random moving surface", Phil. Trans. Roy, Soc. London, vol. A249, pp. 321-387, February 1957.

8. P. Whittle, "On stationary processes in the plane", Biometrika, vol. 41, pp. 434-449, 1954.

9. A. W. Freiberger and U. Grenander, Surface Patterns in Theoretical Geography, Reports on Pattern Analysis, no. 41, Division of Applied Mathematics, Brown University, Providence, RI, September 1976.

10. B. R. Hunt and T. M. Cannon, "Nonstationary assumptions for Gaussian models of images", (Correspondence), IEEE Trans. on Syst., Man, and Cyb., vol. SMC-6, no. 12, pp. 876-882, December 1976.

11. P. Swerling, "Statistical properties of the contours of random surfaces", IRE Trans. on Inf. Th., vol. IT-8, no. 3, pp. 315-321, July 1962.

12. R. Price, "A useful theorem for nonlinear devices having Gaussian inputs", IRE Trans. on Inf. Th., vol. IT-4, no. 2, pp. 69-72, June 1958.

13. R. Price, "Comments on: A useful theorem for nonlinear devices having Gaussian inputs", (Correspondence), IEEE Trans. on Inf. Th., vol. IT-10, no. 2, pp. 171, April 1964.

14. S. O. Rice, "The mathematical analysis of random noise", Bell Syst. Tech. J., vol. 23, pp. 282-332, 1944.

15. S. O. Rice, "The mathematical analysis of random noise", Bell Syst. Tech. J., vol. 24, pp. 46-156, 1945.

16. S. A. Roach, The Theory of Random Clumping, Methuen & Co., London, 1968, Chapter 5.

17. J. T. Tou and Y. S. Chang, "An approach to texture pattern analysis and recognition", Proc. 1976 IEEE Conf. on Decis. and Cont., pp. 398-403, December 1976.

UNCLASSIFIED
SECURITY CLASSIFICATION OF THIS PAGE (When Data Entered)

REPORT DOCUMENTATION PAGE		READ INSTRUCTIONS BEFORE COMPLETING FORM
1. REPORT NUMBER	2. GOVT ACCESSION NO.	3. RECIPIENT'S CATALOG NUMBER
4. TITLE (and Subtitle) STATISTICAL PROPERTIES OF THRESHOLDED IMAGES		5. TYPE OF REPORT & PERIOD COVERED Technical 6. PERFORMING ORG. REPORT NUMBER TR-559 ✓
7. AUTHOR(s) Durga P. Panda		8. CONTRACT OR GRANT NUMBER(s) DAAG53-76C-0138 ✓
9. PERFORMING ORGANIZATION NAME AND ADDRESS Computer Sci. Ctr. ✓ Univ. of Maryland College Park, MD 20742		10. PROGRAM ELEMENT, PROJECT, TASK AREA & WORK UNIT NUMBERS
11. CONTROLLING OFFICE NAME AND ADDRESS U. S. Army Night Vision Lab. Ft. Belvoir, VA 22060		12. REPORT DATE July 1977 13. NUMBER OF PAGES
14. MONITORING AGENCY NAME & ADDRESS(if different from Controlling Office)		15. SECURITY CLASS. (of this report) Unclassified 15a. DECLASSIFICATION/DOWNGRADING SCHEDULE

16. DISTRIBUTION STATEMENT (of this Report)

Approved for public release; distribution unlimited.

17. DISTRIBUTION STATEMENT (of the abstract entered in Block 20, if different from Report)

18. SUPPLEMENTARY NOTES

19. KEY WORDS (Continue on reverse side if necessary and identify by block number)

Thresholding
Connected components
Statistical analysis
Image modelling
Image analysis

20. ABSTRACT (Continue on reverse side if necessary and identify by block number)

The threshold operator is an important operator in image analysis tasks such as segmentation and edge detection. A statistical analysis of the response of this operator is presented in this paper. The input grayscale image is modelled as a two-dimensional homogeneous random process completely characterized by its mean and power spectrum.

DD FORM 1 JAN 73 1473 EDITION OF 1 NOV 65 IS OBSOLETE

UNCLASSIFIED
SECURITY CLASSIFICATION OF THIS PAGE (When Data Entered)